ISSN 1070-3284, Russian Journal of Coordination Chemistry, 2018, Vol. 44, No. 2, pp. 91–102. © Pleiades Publishing, Ltd., 2018.
Original Russian Text © N.V. Gogoleva, G.G. Aleksandrov, A.A. Pavlov, M.A. Kiskin, A.A. Sidorov, I.L. Eremenko, 2018, published in Koordinatsionnaya Khimiya, 2018, Vol. 44, No. 1, pp. 3–13.

Effect of the Structure of Pyridine Ligands and the Substituent in the Carboxylate Anion on the Geometry of Transition Metal Complexes $[M_2(O_2CR)_4L_2]$

N. V. Gogoleva[a], G. G. Aleksandrov[a, †], A. A. Pavlov[b], M. A. Kiskin[a], A. A. Sidorov[a, *], and I. L. Eremenko[a, b]

[a] *Kurnakov Institute of General and Inorganic Chemistry, Russian Academy of Sciences, Moscow, 117907 Russia*
[b] *Nesmeyanov Institute of Organoelement Compounds, Russian Academy of Sciences, Moscow, 117813 Russia*
**e-mail: sidorov@igic.ras.ru*

Received July 10, 2017

Abstract—A series of binuclear tetracarboxylate-linked Mn(II), Fe(II), Co(II), Ni(II), and Cu(II) complexes with 1,2-substituted pyridine, viz., 2,3-cyclododecenopyridine (L), were prepared. Study of the crystal structures of isolated compounds (CIF file CCDC nos. 1575855–1575859) revealed a distortion of the $\{Ni_2(O_2CR)_4L_2\}$ binuclear moiety, manifested as a change in the NiNiN angle (151.67°), in the bridging function of two out of the four carboxylate groups (from μ_2- to (κ^2,μ_2-)), and in the coordination environment of the metal ion (NiO_5N). The results were analyzed in comparison with known data. The magnetic properties of copper(II) and nickel(II) complexes were studied. The copper(II) complex is diamagnetic as a result of strong exchange interactions between the unpaired electrons; in the nickel(II) complex antiferromagnetic exchange interactions were detected ($J_{Ni-Ni} = -25$ cm^{-1}).

Keywords: binuclear complexes, transition metal complexes, steric effect, structure, magnetic properties
DOI: 10.1134/S1070328418020057

INTRODUCTION

Studies of the steric effects in the molecules and crystal packings of coordination compounds are of interest in the context of solving a broad range of fundamental and applied problems. The influence of steric effects of bulky ligands on the composition, structure, and physicochemical parameters of complexes is important for the control over catalytic activity and optical, magnetic, and other properties [1–4].

Binuclear transition metal carboxylates with four identical bridging anions of carboxylic acids containing α-substituted pyridines or other bulky ligands as apical N-donor molecules can be regarded as classical objects for investigation of the role of steric effects in the geometry of complexes [5–18].

An important detail is the presence of bulky substituents in the bridging carboxylate group, which act as a sort of partners participating in non-valence interactions with sterically crowded apical ligands. Apart from the change in the geometry of the metal core with the invariable composition of $[M_2(O_2CR)_4L'_2]$ (M is the 3*d*-metal ion, O_2CR = carboxylate anion, L' = pyridine or its substituted analog), one could also expect changes in the magnetic properties of compounds: enhancement/weakening of the energy of spin–spin exchange interactions between paramagnetic centers, although for systems studied previously, no highly pronounced variation of exchange parameters was observed for the same type structures with identical metal ions.

In this paper, we present the results of a study of the effect of a bulky conformationally mobile substituent, in our case, 2,3-cyclododecenopyridine (L) on the geometry of binuclear 3*d*-metal tetracarboxylates of the general formula $[M_2(\mu\text{-}O_2CR)_4L_2]$ (M = Mn(II), Fe(II), Co(II), Ni(II), and Cu(II)), in which the metal ion forms a tetragonal-pyramidal coordination (which is formally pseudooctahedral, because one coordination site is occupied by the second metal atom, although without the formation of a metal–metal bond). In addition, we analyzed the magnetic behavior of nickel(II) dimers with four carboxylate bridges, whose structure changes when 2,3-cyclododecenopyridine is present as the apical ligand.

EXPERIMENTAL

New compounds were synthesized in air using MeCN (99%), benzene (99%), heptane (99%), and

† Deceased.

hexane (99%). Commercially available chemicals, 2,3-cyclododecenopyridine (L; Aldrich Chemie, >98%), and solvents, were used as received. The initial trimethylacetates, $[Mn(Piv)_2(EtOH)]_n$, $[Fe(Piv)_2]_n$, $[Co(Piv)_2]_n$, $[Ni_9(OH)_6(Piv)_{12}(HPiv)_4]$, and $[Cu_2(Piv)_4(HPiv)_2]$, were prepared by known procedures [19–23].

The IR spectra of complexes were measured on a Perkin Elmer Spectrum 65LS FTIR spectrophotometer using the independent total reflection method. Elemental microanalysis was carried out on a Euro EA-3000 analyzer. Complexes **I** and **II** were synthesized under argon. The ^1H and ^{13}C NMR spectra were recorded on a Bruker Avance 600 NMR spectrometer (Germany). The chemical shifts were referred to the residual signals of the deuterated solvents. The spectra were processed using the Mestrenova 10.0 software.

Synthesis of $M_2(Piv)_4(L)_2$ (M = Mn (I), Fe (II), Co (III), Ni (IV), Cu (V)). Complexes **I**–**V** were prepared by the reaction of the appropriate starting compound, $[Mn(Piv)_2(EtOH)]_n$, $[Fe(Piv)_2]_n$, $[Co(Piv)_2]_n$, $[Ni_9(OH)_6(Piv)_{12}(HPiv)_4]$, or $[Cu_2(Piv)_4(HPiv)_2]$, with a stoichiometric amount of the ligand L in MeCN. The metal salt (2 mmol; 0.22 mmol for Ni and 1 mmol for Cu) and the ligand L (2 mmol) were dissolved in 50 mL of MeCN at 80°C and kept for 40 min. The solutions thus formed (colorless for **I**, yellow for **II**, blue-green for **III**, brown green for **IV**, and light blue for **V**) were concentrated at 80°C to a 10 mL volume and allowed to stand at room temperature for 24 h. The resulting crystals where suitable for X-ray diffraction. For complete isolation of the products, solutions were additionally kept at 5°C for 24 h. The products of the same composition and structure were formed upon the synthesis in benzene (10 mL) with subsequent addition of 50 mL of hexane to decrease the solubility or with subsequent addition of 50 mL of heptane and threefold evaporation of the solution (to 20 mL).

Compound **II** is rapidly oxidized in air both in the solid state and in solution, which prevents determination of the exact composition of the phase and spectral characterization; only the crystal structure was studied for this complex. Complex **I** is oxidized in air when kept for a long time (more than 24 h).

I: yield 0.71 g (75% in relation to the initial amount of $[Mn(Piv)_2(EtOH)]_n$).

For $C_{50}H_{82}N_2O_8Mn_2$

Anal. calcd., %	C, 63.3	H, 8.7	N, 3.0
Found, %	C, 62.7	H, 8.4	N, 2.8

IR (ν, cm^{-1}): 2952 m, 2923 m, 2863 m, 1616 m, 1594 m, 1581 m, 1479 s, 1438 m, 1418 s, 1374 m, 1358 m, 1320 w, 1293 w, 1276 w, 1226 s, 1172 w, 1147 w, 1122 w, 1093 w, 1078 w, 1062 w, 1030 w, 1011 w, 974 w, 935 w, 894 m, 858 w, 839 w, 787 s, 606 s, 530 w, 462 w, 427 s, 418 s, 407 s.

III: yield 0.76 g (80% in relation to the initial amount of $[Co(Piv)_2]_n$).

For $C_{50}H_{82}N_2O_8Co_2$

Anal. calcd., %	C, 62.8	H, 8.6	N, 2.9
Found, %	C, 62.8	H, 8.4	N, 2.8

IR (ν, cm^{-1}): 2951 m, 2923 m, 2863 m, 1617 m, 1594 m, 1582 m, 1480 s, 1438 m, 1417 s, 1374 m, 1358 m, 1319 w, 1291 w, 1275 w, 1226 s, 1170 w, 1147 w, 1122 w, 1093 w, 1078 w, 1062 w, 1030 w, 1011 w, 974 w, 935 w, 894 m, 858 w, 839 w, 787 s, 606 s, 530 w, 462 w, 427 s, 418 s, 407 s.

IV: yield 0.77 g (81% in relation to the initial amount of $[Ni_9(OH)_6(Piv)_{12}(HPiv)_4]$).

For $C_{50}H_{82}N_2O_8Ni_2$

Anal. calcd., %	C, 62.8	H, 8.6	N, 2.9
Found, %	C, 62.7	H, 8.5	N, 2.8

IR (ν, cm^{-1}): 2979 m, 2954 m, 2924 m, 2863 m, 1611 s, 1520 w, 1481 s, 1438 m, 1418 s, 1372 m, 1355 m, 1340 w, 1272 w, 1258 w, 1225 s, 1207 m, 1193 w, 1184 w, 1170 w, 1146 w, 1128 w, 1109 w, 1093 w, 1080 w, 1065 w, 1027 w, 971 w, 935 w, 895 m, 851 w, 800 m, 788 m, 759 m, 741 w, 727 w, 636 w, 611 s, 537 w, 514 w, 504 w, 430 s, 410 m, 403 m.

V: yield 0.82 g (85% in relation to the initial amount of $[Cu_2(Piv)_4(HPiv)_2]$).

For $C_{50}H_{82}N_2O_8Cu_2$

Anal. calcd., %	C, 62.2	H, 8.6	N, 2.9
Found, %	C, 62.0	H, 8.4	N, 2.8

IR (ν, cm^{-1}): 3075 w, 2953 m, 2924 m, 2863 m, 1615 s, 1582 m, 1480 s, 1456 m, 1438 m, 1415 s, 1375 m, 1361 m, 1319 w, 1291 w, 1272 w, 1224 s, 1154 w, 1121 w, 1093 w, 1077 w, 1060 w, 1010 w, 970 w, 936 w, 896 m, 855 w, 839 w, 800 m, 788 s, 761 m, 730 m, 706 w, 617 s, 529 w, 494 w, 440 s, 412 s. ^1H NMR (CD_2Cl_2; δ, ppm): 1.62 (br.s, 4H, CH_2), 1.74 (br.s, 4H, CH_2), 1.80 (br.s, 4H, CH_2), 1.84 (br.s, 4H, CH_2), 2.00 (br.s, 12H, CH_2), 2.61 (br.s, 4H, CH_2), 3.54 (br.s, 36H, CH_3), 3.91 (br.s, 4H, CH_2), 5.25 (br.s, 4H, CH_2), 8.54 (br.s, 2H, *m*-CH), 8.93 (br.s, *p*-2H, CH), 11.35 (br.s, 2H, *o*-CH). ^{13}C NMR (CD_2Cl_2; δ, ppm): 23.61 (s., CH_2), 24.00 (s., CH_2), 26.82 (s., CH_2), 27.47 (s., CH_2), 28.06 (s., CH_2), 28.24 (s., CH_2), 29.48 (br.s, CH_2), 31.16 (s., CH_2), 32.00 (br.s, CH_2), 35.51 (br.s, CH_2), 37.90 (br.s, CH_3), 127.54 (br.s, Ar–C), 139.73 (br.s, Ar–C), 148.46 (br.s, Ar–C), 168.75 (br.s, Ar–C).

The single crystal X-ray diffraction study of complexes **I**–**V** was carried out on a Bruker Apex II dif-

Table 1. Crystallographic parameters and structure refinement details for **I**–**V**

Parameter	Value				
	I	**II**	**III**	**IV**	**V**
Molecular formula	$C_{50}H_{82}N_2O_8Mn_2$	$C_{50}H_{82}N_2O_8Fe_2$	$C_{50}H_{82}N_2O_8Co_2$	$C_{50}H_{82}N_2O_8Ni_2$	$C_{50}H_{82}N_2O_8Cu_2$
M	949.06	950.88	957.04	956.60	966.26
T, K	120(2)	120(2)	120(2)	293(2)	120(2)
System	Triclinic	Monoclinic	Triclinic	Triclinic	Triclinic
Space group	$P\bar{1}$	$P2_1/c$	$P\bar{1}$	$P\bar{1}$	$P\bar{1}$
a Å	9.7338(4)	14.8983(8)	9.6766(11)	9.6725(6)	9.6256(14)
b Å	11.5937(5)	18.1090(9)	11.4279(13)	11.1643(7)	11.568(2)
c Å	13.3803(5)	9.7144(5)	13.642(2)	13.5167(9)	13.271(2)
α, deg	108.5800(10)	90	108.646(2)	110.1990(10)	13.2709(19)
β, deg	100.4510(10)	97.2790(10)	101.258(2)	96.8490(10)	99.467(3)
γ, deg	107.8210(10)	90	108.185(2)	106.9330(10)	108.288(3)
V, Å^3	1295.88(9)	2599.8(2)	1283.0(3)	1270.58(14)	1280.1(3)
Z	1	2	1	1	1
ρ(calcd.), g/cm^3	1.216	1.215	1.239	1.250	1.251
μ, mm^{-1}	0.537	0.608	0.697	0.792	0.881
θ_{max}, deg	30.03	30.00	28.32	33.42	28.28
T_{min}/T_{max}	0.843/0.919	0.815/0.904	0.792/0.897	0.722/0.827	0.766/0.887
Number of measured reflections	14963	23051	9832	20594	9838
Number of unique reflections	7331	7376	5910	9799	5938
Number of reflections with c $I > 2\sigma(I)$	5906	4353	3664	6084	3078
R_{int}	0.026	0.077	0.058	0.054	0.074
Number of refined parameters	280	280	280	280	280
GOOF	1.00	1.00	1.00	0.84	0.85
R_1 ($I > 2\sigma(I)$)	0.070	0.0592	0.052	0.043	0.061
wR_2 ($I > 2\sigma(I)$)	0.211	0.1566	0.114	0.063	0.101

fractometer (CCD detector, MoK_α, λ = 0.71073 Å, graphite monochromator) [24]. A semiempirical absorption correction was applied [25]. The structures were solved by the direct methods and refined in the full-matrix anisotropic approximation for all non-hydrogen atoms. The hydrogen atoms at the carbon atoms of organic ligands were generated geometrically and refined in the "riding" model. The calculations were carried out using the SHELX-97 program package [26]. The crystallographic parameters of **I**–**V** are summarized in Table 1. The full set of X-ray diffraction data for complexes **I**–**V** is deposited with the Cambridge Crystallographic Data Centre (nos. 1575855–1575859; deposit@ccdc.cam.ac.uk or http://www.ccdc.cam.ac.uk/data_request/cif).

Powder X-ray diffraction analysis was carried out on a Bruker D8 Advance powder diffractometer (CuK_α, λ = 1.54 Å, Ni filter, LYNXEYE detector).

The ESR spectra were recorded on an E-680X Elexsys radiospectrometer (Bruker) in the X-range at room temperature.

The magnetic properties of the powders of compounds **IV** and **V** were measured on a PPMS-9 Quantum Design automatic facility for measuring physical properties. The temperature dependences of magnetization were determined in the temperature range T =

9–300 K in an external magnetic field with the strength H = 5 kOe. Corrections for the magnetic properties of the sample holder and compound diamagnetism were applied using the Pascal scheme.

RESULTS AND DISCUSSION

The reaction of 2,3-cyclododecenopyridine (L) with transition metal Mn(II), Fe(II), Co(II), Ni(II), and Cu(II) pivalates (with the L : M ratio of 1 : 1) results in the formation of binuclear tetracarboxylate complexes of the well-known structural type, $[M_2(\mu\text{-Piv})_4L_2]$ (M = Mn (**I**), Fe (**II**), Co (**III**), Ni (**IV**), and Cu (**V**); Piv = pivalate anion). The reactions with nickel(II), cobalt(II), and copper(II) pivalates were carried out in the presence of the atmospheric oxygen, while the manganese(II) and iron(II) complexes were prepared under argon.

The crystallographic parameters and structure refinement details for **I**–**V** are presented in Table 1. In complexes **I** and **III**–**V** with the Mn^{2+}, Fe^{2+}, Co^{2+}, and Cu^{2+} ions (Fig. 1a), the metal ions are linked by four carboxylate bridges. Their coordination environment is supplemented by the N atom of the ligand L to give a square pyramid (τ(Mn) = 0.018, τ(Fe) = 0.009, τ(Co) = 0.003, τ(Cu) = 0 [27]). Nickel(II) complex **IV** is generally similar, but the metal carboxylate core is distorted as a result of chelating bridging coordination giving the Ni···O(3*A*) short contact (2.473 Å) (Fig. 1b). Thus, unlike the previously described centrosymmetric dimeric nickel complexes, $[L_2Ni_2(O_2CR)_4]$ (Table 2) [28–32], in compound **IV**, the sixths site is formally occupied by an additional oxygen atom, and the environment of the metal ion thus becomes pseudooctahedral. It is noteworthy that the distortions of the square pyramidal coordination environment in complexes **I**, **III**–**V** are similar (except for the nickel complex **IV**). The pyramid base generally retains the square shape, as indicated by the close values for the OMO angles formed by the neighboring metal-coordinated oxygen atoms and the metal atom (Table 2). The OMN angles show that the axial vertex of the pyramid is deflected from the normal to the point of intersection of diagonals, which is caused by the effect of the bulky substituent in the α-position of the pyridine moiety. For each metal complex **I**–**V**, the difference between the OMO and OMN angles is 3°–7°. The M–O and M–N bond lengths are usual and are given below in the description of the structures of complexes. The most interesting consequence of the steric strain created by the substituent in ligand L is the non-equivalence of the COM angles and the deviation of the N–M–M–N moiety from linearity, which is characterized by the deflection of the NMM angle from 180°. Below we compare these two geometric parameters for the molecule containing a particular metal and other known complexes of the same metal.

Analysis of the geometry of the N–M···M–N moiety in binuclear carboxylates shows that the NMM' angle tends to deviate from 180° by 10°–30° (Table 2), depending on the geometric characteristics of ligand L. In the series of dimers **I**–**V**, the greatest deviation is inherent in the NNiNi angle in **IV** (Table 1, entries 14–22 [28–32]), as compared with the corresponding angles in dimers **I**–**III** and **V** in other transition metals or analogous compounds with other carboxylate bridges and with α-substituted pyridines (2,3-lutidine, 2-amino-5-methylpyridine, and so on) as the apical ligands [30–39] (Table 2).

The non-equivalence of the CNM angles in the new dimers **I**–**V** with the apical ligand L is approximately the same as in other $[M_2(Piv)_4]L_2$ complexes with bulky apical substituents, e.g., 2,3-lutidine [29, 31, 34]. The distortions of the metal carboxylate core upon the coordination of L are not higher than those in the case of α-methyl- or aminopyridine (Table 3), although increasing steric strain in the dimer molecule caused by the presence of a particular α-substituent in the pyridine ligand could even be expected to prevent the ligand binding to the metal.

The manganese compounds $[Mn_2(O_2CR)_4L'_2]$ (L' = pyridine derivative) with the monodentate ligand L are represented by only a few pivalate complexes. In the case of L, the Mn···Mn distance decreases by ~0.1 Å and the N–Mn···Mn–N moiety deviates from the linearity (the NMnMn decreases by 13°–19°). The Mn atom forms a distorted tetragonal-pyramidal coordination (Table 2). The Mn–O (2.030(2)–2.089(2) Å) and Mn–N (2.166(2) Å) bond lengths are typical of this type of Mn(II) complexes [15, 28, 29]. As can be seen from the following, the response of the $\{Mn_2(O_2CR)_4\}$ metal core to the steric strain of the bulky substituent in the ligand L is approximately the same as in the case of cobalt. However, unlike the cobalt and iron complexes, the Mn···Mn distance is somewhat shorter than for other pivalate complexes. Although the small number of structurally characterized $[L_2Mn_2(O_2CR)_4]$ complexes does not allow serious conclusions to be drawn, it can be noted that out of the considered metals, only manganese is capable of forming complexes of the given composition with chelating ligands [53]. In such complexes, four carboxylate bridging anions link two manganese atoms located in the octahedral environment. This is provided by the rotation and shift of the square $\{MnO_4\}$ units relative to each other. This operation transfers the bridging carboxylate groups into a different conformation and increases the Mn···Mn distance to 3.61 Å. The ability of manganese to form structures of this type might be indicative of the highest conformational mobility in the series of considered complexes. Unfortunately, it is impossible to gain this information for the element located ahead of manganese in the transition metal

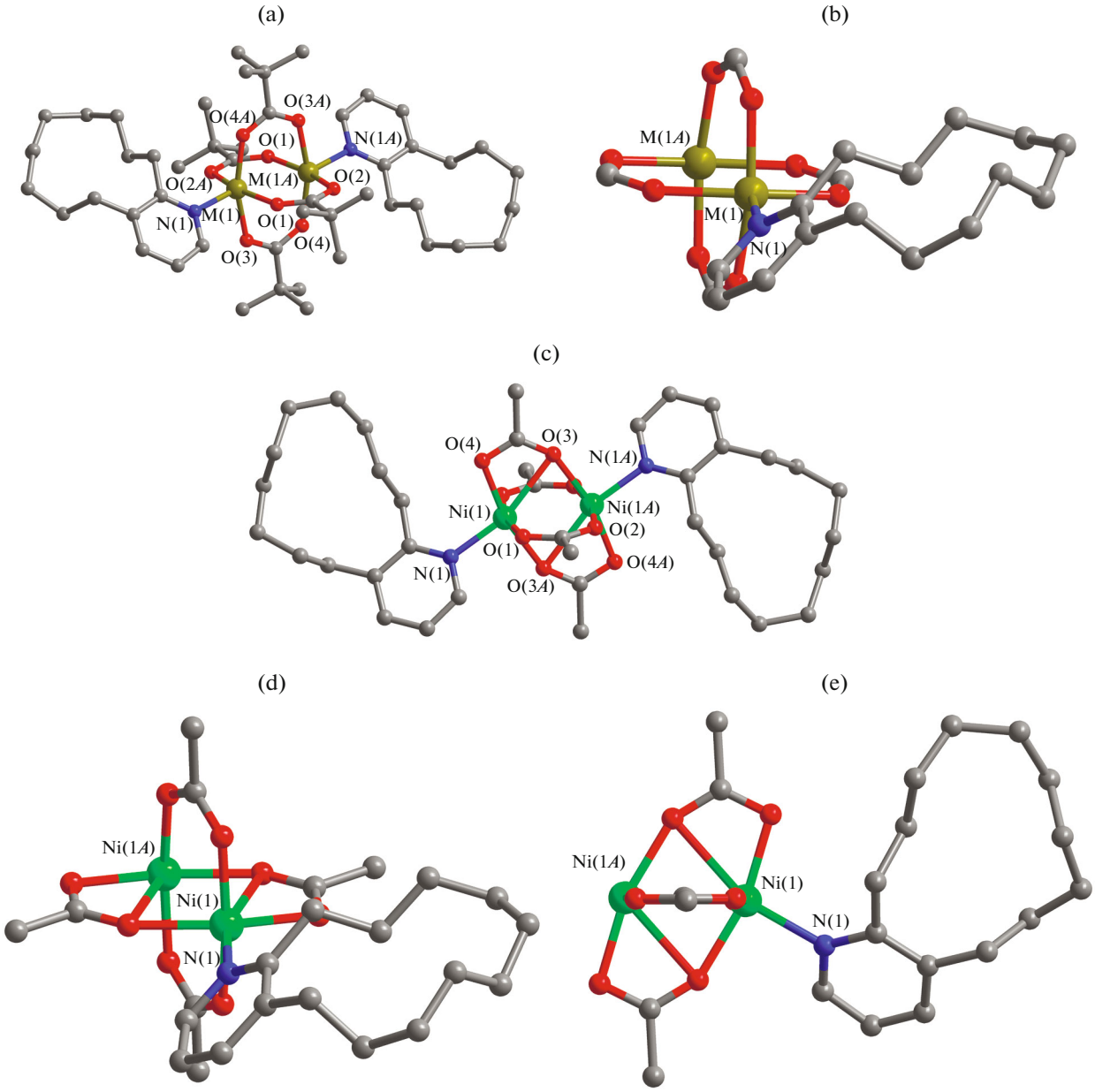

Fig. 1. (a) General structure of the complexes $[M_2(Piv)_4L_2]$, where M is Mn, Fe, Co, Cu, hydrogen atoms are omitted; (b) illustration of the position of 2,3-cyclododecenopyridine relative to the $\{M_2(\mu_2\text{-}O_2C)_4\}$ moiety; (c) structure of the $[Ni_2(Piv)_4L_2]$ complex, hydrogen atoms and the *tert*-butyl groups are omitted; (d) illustration of the position of 2,3-cyclododecenopyridine relative to the $\{Ni_2(\mu_2\text{-}O_2C)_2(\mu_2\text{-}O_2C)_2(\kappa^2,\mu_2\text{-}O_2C)_2\}$ moiety; (e) illustration of the position of 2,3-cyclododecenopyridine relative to the planar $\{Ni_2(\kappa^2,\mu_2\text{-}O_2C)_2\}$ moiety.

series, because chromium forms the formally quadruple metal–metal bond in this type of structures [54].

In the iron(II) complex **II**, the N–Fe–Fe–N moiety is more linear (2.217(2) Å) and the Fe···Fe distance is somewhat longer (Table 3) as compared with the other few known complexes with alkyl α-substituents. Apparently, this reduces the steric strain, because the FeFeN angle is even smaller than in the case of less bulky substituents. The Fe–O bond lengths in **II** (2.098(2)–2.140(2) Å) have similar values and are typical of Fe(II) carboxylates. The virtually linear arrangement of the N–Fe–Fe–N atoms in the pivalate complex with 2,6-diaminopyridine is caused by the influence of intramolecular hydrogen bonds [36]. For the same reason, The Fe–N bond length in this compound has a usual value, unlike that in the rhodium complex of a similar composition [55], in which this bond increases by approximately 0.3 Å.

In the cobalt(II) complex **III**, the role of steric strain created by the substituent of ligand L cannot be

Table 2. Selected interatomic distances and bond angles in complexes **I**–**V**

Complex	I	II	III	IV	V
Bond, Å					
M–O	2.029(2)	2.098(2)	2.001(2)	2.0004(10)	1.951(3)
	2.064(2)	2.110(2)	2.015(2)	2.0137(10)	1.959(3)
	2.066(2)	2.110(2)	2.032(2)	2.0214(10)	1.963(3)
	2.090(2)	2.140(2)	2.070(2)	2.0825(10)	1.965(3)
M–N	2.166(2)	2.217(2)	2.102(2)	2.0504(12)	2.251(3)
M···M	2.8916(6)	3.111(2)	2.8233(8)	2.7161(4)	2.6615(9)
Angle, deg					
OMO	90.01(11)	155.04(9)	92.43(10)	166.43(4)	89.26(13)
	160.95(10)	89.62(8)	162.57(9)	91.67(4)	89.64(13)
	87.28(10)	87.46(8)	89.29(9)	90.22(4)	166.87(10)
	88.66(11)	84.75(8)	87.94(9)	87.61(4)	166.89(10)
	161.15(10)	87.73(8)	162.81(9)	87.17(4)	89.25(13)
	87.87(10)	155.56(8)	85.38(10)	165.31(4)	88.86(13)
OMN	107.19(9)	102.20(8)	104.35(9)	99.45(5)	102.02(11)
	111.08(9)	102.19(8)	107.11(10)	93.19(4)	88.53(10)
	91.34(8)	108.86(8)	91.67(9)	103.14(5)	104.49(10)
	87.23(9)	95.58(8)	89.40(9)	91.45(5)	90.96(11)
NMM	161.15(6)	169.5(4)	161.58(7)	151.67(4)	168.35(8)
COM	133.2(2)	127.2(2)	135.8(2)	123.07(9)	127.1(2)
	120.8(2)	129.8(2)	116.1(2)	124.50(9)	121.4(2)
	125.2(2)	118.2(2)	123.9(2)	152.09(11)	123.5(3)
	128.7(2)	142.3(2)	128.2(2)	100.12(9)	125.0(3)
CNM	114.5(2)	111.8(2)	126.5(2)	112.70(10)	129.3(2)
	125.8(2)	128.8(2)	114.7(2)	127.89(10)	111.6(2)
OCO	124.6(3)	125.1(2)	124.6(3)	125.84(14)	124.5(3)
	125.0(2)	124.1(2)	125.2(3)	122.40(14)	124.6(4)

followed, because the distortions of the metal core are approximately the same as in other known compounds with axial 2-amino-5-methylpyridine or 2,6-diaminopyridine molecule [37] and are the same as in the case of unsubstituted pyridine [38] (Table 3). The Co–O (2.001(4)–2.067(4) Å) and Co–N (2.111(4) Å) bond lengths in **III** are typical of cobalt(II) carboxylates.

All known nickel complexes with α-substituted pyridines have rather similar Ni···Ni distances and a moderate range of NiNiN angles (Table 2). The Ni–O (2.000(1)–2.083(1) Å) and Ni–N (2.050(1) Å) distances in **IV** are typical of nickel(II) carboxylates; however, as noted above, compound **IV** is characterized by the most pronounced deviation from linearity in the N–Ni···Ni–N moiety (the NiNiN angle decreases to 151.67(4)°, and the short Ni···O(3*A*) contact of 2.473 Å appears). Formally, the environment of nickel can be regarded as a $\{NiNO_5\}$ distorted octahedron. The pyridine ring plane is rotated relative to the plane containing the chelating bridging carboxylate groups through 42.82(4)°. Thus, the pyridine moiety occupies a position that is virtually equivalent with respect to the most proximate carboxylate groups. However, because of the steric effect of the bulky substituents, only two carboxylate groups located in the same plane are highly distorted (one NiOC angle increases to 152.09(11)°, while the other one decreases to 100.12(9)°) (Figs. 1c, 1e). This results in a considerable displacement of the whole Ni–O–C group and actually in the transition to a chelating bridging coordination. The other two carboxylate groups, which occupy typical bridging positions, have nearly equal NiOC angles. For the Mn (**I**), Fe (**II**), Co (**III**), and Cu (**V**) complexes, the geometric distortions of the bridging carboxylate groups are an order of magnitude less pronounced than those in the Ni complex (**IV**), although the trends are the same.

Table 3. Comparison of key geometric characteristics of some binuclear complexes with the $\{M_2(\mu\text{-}O_2CR)_4\}$ unit

Entry	Compound	Bond		NMM' or OMM' angle, deg	Ref.
		M–N, Å	M···M, Å		
1	$[Mn_2(Piv)_4L_2]$ (**I**)	2.166(2)	2.8916(6)	161.16(6)	This work
2	$[Mn_2(Piv)_4(2,3\text{-}Lut)_2]$	2.183 2.179	3.065 3.055	173.71 174.74 177.96 177.96	32
3	$[Mn_2(Piv)_4(2,6\text{-}(NH_2)_2\text{-}Py)_2]$	2.180	3.088	180.00	33
4	$Mn_2(Piv)_4(2,6\text{-}(NH_2)_2\text{-}Py)_2]$ $Mn_2(Piv)_4(2,6\text{-}(NH_2)_2\text{-}Py)_2]$, another phase	2.222 2.179	3.119 3.057	178.11 176.53	33
6	$[Fe_2(Piv)_4L_2]$ (**II**)	2.217(2)	3.111(2)	169.5(4)	This work
7	$[Fe_2(Piv)_4(2,3\text{-}Lut)_2]$	2.135	2.866	164.91	34
8	$[Fe_2(Piv)_4(2\text{-}Me\text{-}Py)_2]$	2.128	2.858	166.53	35
9	$[Fe_2(Piv)_4(2,6\text{-}(NH_2)_2\text{-}Py)_2$	2.169 2.157	2.936 2.938	178.72 175.52	36
10	$[Co_2(Piv)_4L_2]$ (**III**)	2.102(2)	2.8233(8)	161.55(7)	This work
11	$[Co_2(Piv)_4(5\text{-}Me\text{-}2\text{-}NH_2\text{-}Py)_2]$	2.066	2.748	170.58	37
		2.071	2.865	160.84	
12	$[Co_2(Piv)_4(2,6\text{-}(NH_2)_2\text{-}Py)_2]$	2.109	2.926	175.10	37
13	$[Co_2(Piv)_4(Py)_2]$	2.067 2.071	2.734(1) 2.770(1)	160 168	39
14	$[Ni_2(Piv)_4L_2]$ (**IV**)	2.0504(12)	2.7161(4)	151.67(4)	This work
15	$[Ni_2(Piv)_4(2,4\text{-}Lut)_2]$	2.030	2.708	166.65	28
16	$[Ni_2(Piv)_4(2\text{-}Me\text{-}Py)_2]$	2.037	2.717	169.46	28
17	$[Ni_2(Piv)_4(2,5\text{-}Lut)_2]$	2.033	2.720	160.84	28
18	$[Ni_2(Piv)_4(2\text{-}Et\text{-}Py)_2]$	2.042	2.723	166.00	28
19	$[Ni_2(Piv)_4(2,3\text{-}Lut)_2]$	2.045	2.741	168.3	29
20	$[Ni_2(Piv)_4(Et_3N)_2]$	2.106	2.728	177.7	29
21	$[Ni_2(Bzo)_4(2,3\text{-}Lut)_2]$	2.044	2.720	152.23	31
22	$[Ni_2(1\text{-}Naph)_4(2,3\text{-}Lut)_2]$	2.035	2.683	171.12	32
23	$[Cu_2(Piv)_4L_2]$ (**V**)	2.251(3)	2.6615(9)	168.37(8)	This work
24	$[Cu_2(Piv)_4(2,6\text{-}Lut)_2]$	2.360	2.722	178.18	39
25	$[Cu_2(Piv)_4(2\text{-}Me\text{-}6\text{-}NH_2\text{-}Py)_2]$	2.295	2.730	177.14	40
26	$[Cu_2(Piv)_4(2,6\text{-}NH_2\text{-}Py)_2]$	2.243 2.762	2.762	179.81 179.64	40
27	$[Cu_2(Piv)_4(2,6\text{-}NH_2\text{-}Py)_2] \cdot [Cu_2(Piv)_4(CH_3CN)_2]$	2.272	2.706	177.83	40

Table 3. (Contd.)

Entry	Compound	Bond		NMM' or OMM' angle, deg	Ref.
		M–N, Å	M···M, Å		
28	$[Cu_2(OOCC(Me)_2Ph)_4(2,6\text{-Lut})_2]$	2.306 2.286	2.907	180.00	41
29	$[Cu_2(O_2CH_2C(Me)_3)_4(2\text{-Me-Py})_2]$	2.238	2.666	174.41	42
30	$[Cu_2(O_2CMe)_4(2\text{-Me-Py})_2]$	2.246	2.673	175.68	43
31	$[Cu_2(O_2CMe)_4(2\text{-CN-Py})_2]$	2.235	2.600	176.10	44
32	$[Cu_2(O_2CPh)_4(2,6\text{-Lut})_2]$	2.283	2.723	176.64	45
33	$[Cu_2(2\text{-Naph})_4(2,3\text{-Lut})_2]$	2.176	2.706	175.79	32
34	$[Cu_2(O_2CH_2Cl)_4(2\text{-Me-Py})_2]$	2.162	2.747	175.26	46
35	$[Cu_2(O_2CCCl_3)_4(2\text{-}ClH_2CH_2\text{-Py})_2]$	2.242	2.630	170.48	47
36	$[Cu_2(O_2CCCl_3)_4(2\text{-Et-Py})_2]$	2.031 2.033	3.261	152.59 156.14	48
37	$[Cu_2(O_2CCCl_3)_4(2,3\text{-Lut})_2]$	2.019	3.216	161.87 162.32	48
38	$[Cu_2(O_2CCCl_3)_4(2,5\text{-Lut})_2]$	2.007 2.016	3.226	157.72 163.26	48
40	$[Cu_2(Piv)_4\{O(CH_2\text{-}C_6H_5)_2\}_2]$	2.196 2.177	2.569	177.96 176.10	49
41	$[Cu_2(O_2CPh)_4\{O(CH_2\text{-}C_6H_5)_2\}_2]$	2.204 2.219	2.581	175.22 174.81	49
42	$[Cu_2(O_2CCF_3)_4\{O(CH_2\text{-}_6H_5)_2\}_2]$	2.107	2.688	180.00	49
43	$[Cu_2(Piv)_4(THF)_2]$	2.226	2.575	179.49	50
44	$[Cu_2(O_2CMe)_4(THF)_2]$	2.286	2.540	175.20	51
45	$[Cu_2(O_2CMe)_4(THF)_2]$	2.214	2.587	175.92	52

A situation of the same type has been observed previously for the complex $[Ni_2(Bzo)_4(2,3\text{-Lut})_2]$ (**VI**), where Bzo = 3,5-di-*tert*-butylbenzoate anion [16]. A similar distortion of the dimeric moiety was noted, with the arising Ni···O short contact (2.482 Å) involving one of the oxygen atoms of the bridging carboxylate group being close to that found in **V**. This takes place despite the fact that the *tert*-butyl groups in 3,5-di-*tert*-butylphenyl substituents in the carboxylate bridges in **VI** are much more remote from the coordinated 2,3-lutidine molecule [31] than in the case of known pivalate complexes with α-substituted pyridines [28, 29], in which the geometric distortion of the $\{Ni_2((\mu_2\text{-}O_2C)_4\}$ metal core is much less pronounced (Table 3, entries 15–20). Analysis of the known dimeric nickel pivalates with substituted pyridines in the apical positions indicates that the deviation from linearity in the N–Ni···Ni–N moiety of these complexes is in the 166°–170° range, the angle decreasing as follows: 2-methylpyridine, 169.46° [28]; 2,3-lutidine, 168.3° [29]; 2,4-lutidine, 166.65° [28]; and 2,5-lutidine, 160.84° [29]. This attests to a strong influence of intra- and intermolecular interactions, the nature of which is fairly difficult to derive from structural data. Probably, theoretical calculations could be helpful for interpreting the observed changes in the above-noted molecules. Now we can only state that bulky conformationally mobile moieties in a remote position can also have a considerable effect on the NNiNi angle in the $\{Ni_2(\mu\text{-}O_2CR)_4L_2\}$ moiety, whose geometry proved to be sensitive to the nature of neutral N-donor ligands and substituents of the monocarboxylate anions.

In some cases, conditions for noticeable change of the Ni···Ni distance in dimeric carboxylates with nickel atoms have been established. Indeed, in the tri-

ethylamine complex, the distance between the nickel(II) ions somewhat increases, as well as the N–Ni bond length (Table 3), probably due to the large NC_3 Tolman angle (142°) at the triethylamine ligand. Finally, the coordinated Et_3N molecule moves away from the nickel ion, which facilitates the relief of steric strain, and the N–Ni···Ni–N moiety becomes virtually linear (the NNiNi angle is 177.7°). However, in the absence of steric strain, for example, in the nickel pivalate complex with pyridine, the Ni···Ni distance decreases to 2.603 Å with the linearity of the N–Ni···Ni group being retained (the NNiNi angle is 176.8°) [30]. The decrease in the Ni···Ni distance is not inherent in all complexes of this type with pyridine without α-substituents. For instance, in the pyridine-containing nickel complex with the 2,6-*para*-ditolylbenzoate anions, $[Ni_2(2,6\text{-}(p\text{-Tol})_2C_6H_3C_2)_4(Py)_2]$, the steric strain of substituents in the carboxylate anion induces a sharp increase in the Ni···Ni distance (to 2.892 Å) [56].

In the known copper complexes with α-substituted pyridines, the geometric parameters of the $\{L_2Cu_2(\mu\text{-}O_2CR)_4\}$ metal core are similar. The distinction of the structure of complex **V** is the markedly more pronounced deviation from linearity in the N–Cu···Cu–N moiety (Table 2). The Cu–O (1.952(3)–1.966(3) Å) and Cu–N (2.252(3) Å) bond lengths are typical of copper(II) carboxylates [39–52]. A smaller NCuCu angle has been found only in complexes with trichloroacetate anions, but the Cu···Cu distance is the longest and reaches 3.22–3.26 Å (Table 3), while the Cu–N bond is shortened to almost 2 Å [48]. Quite unexpected in this case is the already mentioned outcome of replacement of a hydrogen atom in the coordinated 2-ethylpyridine molecule by chlorine, in particular, in the trichloroacetate complex with coordinated 2-(2-chloroethyl)pyridine, the Cu···Cu distance decreases by 0.5 Å and the Cu–N bond is elongated by 0.2 Å (Table 2) [40].

The fact that according to magnetic measurements, copper(II) complex **V** in the solid state is diamagnetic can be considered as unexpected. At room temperature, the exchange interaction parameters are so high that the two unpaired electrons of two copper(II) ions ($S = 1/2$) in the molecule of the complex are paired ($2J > 1000$ cm^{-1}). This was observed for samples isolated after different syntheses whose phase composition was always determined by powder X-ray diffraction. The ESR spectra of a solid sample and a CH_2Cl_2 solution were characteristic of systems in the triplet state (copper dimers) with the total spin $S = 1$, which is caused by strong exchange interactions between the metal ions [57] and supports the results of magnetic measurements (the results of ESR spectroscopy will be published elsewhere). The presence of the paramagnetic component detected by NMR for a CH_2Cl_2 solution of the complex is, most likely, caused by the presence of the monomer impurity, which is also detected by ESR.

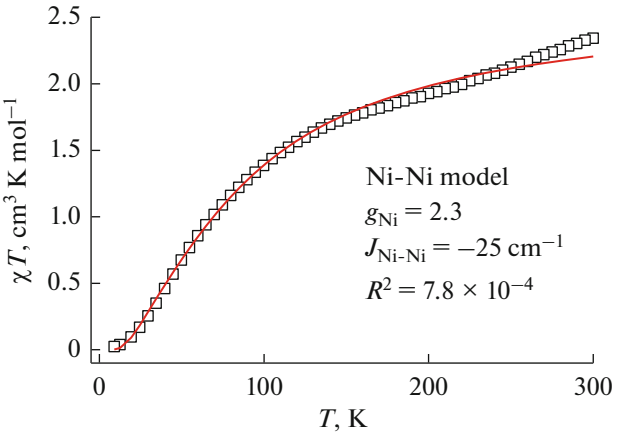

Fig. 2. Magnetic properties of complex **IV** and calculated data (continuous line).

The found geometry changes of the metal tetracarboxylate core of **IV** and the unusual magnetic data for known complex **VI** (sharp decrease in the exchange parameter $-2J$ compared with those of other dimeric nickel carboxylates (Table 4)) with a similar geometry of the core stimulated the effort to measure the magnetic characteristics of **IV**. It was found that the $\chi_M T$ value of the nickel complex **IV** monotonically decreases (from 2.343 to 0.024 cm^3 K mol^{-1}) as the temperature decreases from 300 to 9 K in the field $H = 0.5$ kOe (Fig. 2). The $\chi_M T$ value at room temperature is somewhat lower than the value calculated for two non-interacting ions (2 cm^3 K mol^{-1}), which may indicate that the *g*-factor differs from 2. The pattern of the $\chi_M T(T)$ curve points to antiferromagnetic exchange interactions between the Ni^{2+} ions.

The experimental $\chi_M T(T)$ curve for **IV** was interpreted on the basis of the isotropic spin Hamiltonian for two (1) magnetically equivalent nuclei with the spin $S = 1$:

$$\hat{H} = -2J_{12}S_1S_2 + \beta H(g_1S_1 + g_2S_2),$$

where $J_{12} = J_{Ni-Ni}$, $g_1 = g = g_{Ni}$. The calculation was carried out by full-matrix diagonalization using the Mjöllnir program [58–60]. The best fit between the calculated and experimental $\chi_M T$ dependences on T for **IV** was attained for $J_{Ni-Ni} = -25$ cm^{-1}, $g_{Ni} = 2.30$ ($R^2 = 7.8 \times 10^{-4}$) (Fig. 2). The J_{Ni-Ni} value for **IV** is an order of magnitude lower than the known values for binuclear nickel complexes in which the NiNiN angle approaches 180° and is close to that found in complex **VI** with a similar metal core geometry (Table 4).

The obtained results, together with published data (Table 4) suggest that the J_{Ni-Ni} value in the binuclear tetrabridged carboxylates with nickel(II) ions is correlated with the geometric characteristics of the mag-

Table 4. Geometric characteristics and results of approximation of magnetochemical data for known binuclear nickel(II) complexes of the general formula $[Ni_2(O_2CR)_4L_2]$

Complex*	d(Ni···Ni), Å	NiNiN angle, deg	g_{Ni}	J_{Ni-Ni}, cm^{-1}	Ref.
$[Ni_2(Piv)_4(MetQuin)_2]$	2.754			−160	8
$[Ni_2(Piv)_4(2,4\text{-Lut})_2]$**	2.708	166.65	2.40[a]	−194[a]	28
			2.72[b]	−224[b]	
$[Ni_2(Piv)_4(2,5\text{-Lut})_2]$	2.708	166.65	2.38	−128	28
$[Ni_2(Piv)_4(EtPy)_2]$	2.723	166.00	2.85	−221	28, 29
$[Ni_2(Et_2CHCO_2)_4(Quin)_2]$			2.35	−216	28
$[Ni_2(Me_2PhCCO_2)_4(PPh_3)_2]$	2.752[c]	172.42[c]	2.00	−206	61
	2.765	166.64			
$[Ni_2(Me_2PhCCO_2)_4(Quin)_2]$	2.734	165.70	2.03	−142	29, 61
$[Ni_2(Piv)_4(2\text{-Pic})_2]$	2.717	169.46	2.28	−223	29, 61
$[Ni_2(Piv)_4(Py)_2]$	2.604	176.7	2.175	−130	30, 62
$[Ni_2(PhCO_2)_4(NITpPy)_2]$	2.6454	172.9	2.02	−29.45	63
$[Ni_2(Atc)_4(Py)_2]$	2.700[d]	171.9[d]	2.20	−537	64
	2.651	175.2			
$[Ni_2(L)_2(4,4'\text{-Bipy})_2]$ (H_2L = 2,4-dibenzoylisophthalic acid)	2.700	180.0	2.20	−103.56	65
$[Ni_2(Dpa)_2(MeOH)_2]$ (H_2Dpa = diphenic acid)	2.582	167.8	2.2	−103	66
$[Ni_2(RCOO)_4(4,4'\text{-Bipy})_2]$ (RCOOH = 4,4'-pyridine-2,6-diyl-diisophthalic acid)	2.694	165.17	2.26	−190.03	67
$[Ni_2(Bzo)_4(2,3\text{-Lut})_2]$	2.720	152.23	2.35	−30	31
$[Ni_2(Piv)_4L_2]$ (**IV**)	2.716	151.67	2.30	−25	This work

* Metquin = 2-methylquinoline; Quin = quinoline; 2-Pic = 2-picoline; NITpPy = 2-(4-pyridyl)-4,4,5,5-tetramethylimidazolin-1-oxyl 3-oxide; Atc = 9-anthracenecarboxylate anion.

** The exchange interaction parameters for this complex were calculated using two mathematical models for low-temperature (a) and high-temperature regions (b); Ni···Ni interatomic distances and NiNiP angles in two independent molecules of the complex (c) and in two independent molecules of the complex (d).

netically active $\{Ni(\mu\text{-}O_2CR)_4Ni\}$ moiety. Considering our results and known data, one can assume that steric effects can be utilized as an important tool for controlling the magnetic properties of the dinickel tetracarboxylate moiety taking account of the geometry of the apical ligand.

The new results presented in the paper and the previously obtained data lead to the conclusion that the conformationally mobile binuclear 3*d*-metal complexes $LM(\mu\text{-}O_2CR)_4ML$ are highly sensitive to various intramolecular and intermolecular non-valence contacts. Among α-substituted pyridines, the greatest steric effects have so far been detected for 2,3-cyclododecenopyridine. Similar results come from the use of bulky conformationally mobile carboxylate anions with no steric hindrance to free rotation around the C–C bond for the substituent in the carboxyl group. In the geometry of complexes, the steric strain is mainly manifested as a deviation from linearity in the N–M–M–N moiety and a change in the M···M distance. These changes have specific features for each of the considered metals and, as shown in relation to nickel derivatives, can be used to control the magnetic characteristics of complexes.

ACKNOWLEDGMENTS

The single crystal and powder X-ray diffraction measurements, spectroscopic studies, elemental analysis, and magnetic measurements were carried out at the Collective Use Center of the Kurnakov Institute of General and Inorganic Chemistry, Russian Academy of Sciences.

This work was supported by the Presidium of the Russian Academy of Sciences and the Federal Agency of Scientific Organizations.

REFERENCES

1. Krompiec, S., Penkala, M., Szczubialka, K., and Kowalska, E., *Coord. Chem. Rev.*, 2012, vol. 256, p. 2057.
2. Temkin, O.N., *Homogeneous Catalysis with Metal Complexes: Kinetic Aspects and Mechanisms*, Chichester: Wiley, 2012.
3. Gupta, K.C. and Sutar, A.K., *Coord. Chem. Rev.*, 2008, vol. 252, p. 1420.
4. Seo, J.S., Whang, D., Lee, H., et al., *Nature*, 2000, vol. 404, p. 982.
5. Catterick, J. and Thornton, P., *Adv. Inorg. Chem. Radiochem.*, 1977, vol. 20, p. 291.
6. Catterick, J., Hursthouse, M.D., Thornton, P., and Welch, A.J., *J. Chem. Soc., Dalton Trans.*, 1977, p. 223.
7. Pasynskii, A.A., *Doctoral (Chem.) Dissertation*, Moscow, 1978.
8. Kirillova, N.I., Struchkov, Yu.T., Porai-Koshits, M.A., et al., *Inorg. Chim. Acta*, 1980, vol. 42, p. 115.
9. Novotortsev, V.M., Rakitin, Yu.V., Pasynskii, A.A., and Kalinnikov, V.T., *Dokl. Akad. Nauk SSSR*, 1978, vol. 240, p. 355.
10. Pasynskii, A.A., Eremenko, I.L., Idrisov, T.Ch., and Kalinnikov, V.T., *Koord. Khim.*, 1977, vol. 3, p. 1205.
11. Rakitin, Yu.V., Pasynskii, A.A., Idrisov, T.Ch., et al., *Koord. Khim.*, 1977, vol. 3, p. 807.
12. Pasynskii, A.A., Idrisov, T.Ch., Suvorova, K.M., and Kalinnikov, V.T., *Koord. Khim.*, 1976, vol. 2, p. 1060.
13. Pasynskii, A.A., Eremenko, I.L., Idrisov, T.Ch., and Kalinnikov, V.T., *Koord. Khim.*, 1976, vol. 2, p. 331.
14. Pasynskii, A.A., Idrisov, T.Ch., and Idrisov, T.Ch., *Koord. Khim.*, 1975, vol. 1, p. 1059.
15. Pasynskii, A.A., Idrisov, T.Ch., Suvorova, K.M., et al., *Koord. Khim.*, 1975, vol. 1, p. 799.
16. Pasynskii, A.A., Idrisov, T.Ch., Suvorova, K.M., et al., *Dokl. Akad. Nauk SSSR*, 1978, vol. 220, p. 881.
17. Kirilova, N.I., Gusev, A.I., Pasynskii, A.A., and Struchkov, Yu.T., *Zh. Strukt. Khim.*, 1972, vol. 13, p. 880.
18. Larin, G.M., Kalinnikov, V.T., Aleksandrov, G.G., et al., *J. Organomet. Chem.*, 1971, vol. 27, p. 53.
19. Kiskin, M.A., Fomina, I.G., Aleksandrov, G.G., et al., *Inorg. Chem. Commun.*, 2004, vol. 8, p. 89.
20. Eremenko, I.L., Kiskin, M.A., Fomina, I.G., et al., *J. Cluster Sci.*, 2005, vol. 16, p. 331.
21. Golubnichaya, M.A., Sidorov, A.A., Fomina, I.G., et al., *Izv. Akad. Nauk. Ser. Khim.*, 1999, p. 1773.
22. Eremenko, I.L., Golubnichaya, M.A., Nefedov, S.E., et al., *Izv. Akad. Nauk., Ser. Khim.*, 1998, p. 725.
23. Denisova, T.O., Amel'chenkova, E.V., Pruss, I.V., et al., *Russ. J. Inorg. Chem.*, 2006, vol. 51, no. 7, p. 1020.
24. *SMART (control) and SAINT (integration) Software. Version 5.0*, Madison: Bruker AXS Inc., 1997.
25. Sheldrick, G.M., *SADABS. Program for Scanning and Correction of Area Detector Data*, Göttingen: Univ. of Göttingen, 2004.
26. Sheldrick, G.M., *Acta Crystallogr.*, *Sect. A: Found. Crystallogr.*, 2008, vol. 64, p. 112.
27. Addison, A.W. and Rao, T.N., *J. Chem. Soc., Dalton Trans.*, 1984, p. 1349.
28. Hirashima, N., Husebye, S., Kato, M., et al., *Acta Chem. Scand.*, 1990, vol. 44, p. 984.
29. Morooka, M., Ohba, S., Nakashima, M., et al., *Acta Crystallogr., Sect. C: Cryst. Struct. Commun.*, 1992, vol. 48, p. 1888.
30. Eremenko, I.L., Nefedov, S.E., Sidorov, A.A., et al., *Inorg. Chem.*, 1999, vol. 38, p. 3764.
31. Nikolaevskii, S.A., Kiskin, M.A., Starikova, A.A., et al., *Izv. Akad. Nauk., Ser. Khim.*, 2016, p. 2812.
32. Goldberg, A.E., Kiskin, M.A., Nikolaevskii, S.A., et al., *Russ. J. Coord. Chem.*, 2015, vol. 41, p. 182.
33. Fomina, I.G., Dobrokhotova, Zh.V., Kiskin, M.A., et al., *Izv. Akad. Nauk. Ser. Khim.,* 2007, p. 1650.
34. Sidorov, A.A., Fomina I.G., Aleksandrov G.G., et al., *Izv. Akad. Nauk, Ser. Khim.*, 2004, p. 460.
35. Overgaard, J., Timco, G.A., and Larsen, F.K., *Acta Crystallogr., Sect. E: Struct. Rep. Online*, 2008, vol. 64, p. m497.
36. Eremenko, I.L., Kiskin, M.A., Fomina, I.G., et al., *J. Cluster Sci.*, 2005, vol. 16, p. 331.
37. Pakhmutova, E.V., Malkov, A.E., Mikhailova, T.B., et al., *Izv. Akad. Nauk. Ser. Khim.*, 2003, p. 2006.
38. Golubnichaya, M.A., Sidorov, A.A., Fomina, I.G., et al., *Russ. J. Inorg. Chem.*, 1999, vol. 44, p. 1401.
39. Kani, Y., Tsuchimoto, M., Ohba, S., et al., *Acta Crystallogr., Sect. C: Cryst. Struct. Commun.*, 2000, vol. 56, p. 923.
40. Fomina, I.G., Dobrokhotova, Zh.V., Aleksandrov, G.G., et al., *Izv. Akad. Nauk., Ser. Khim.*, 2007, p. 1660.
41. Goto, M., Kani, Y., Tsuchimoto, M., et al., *Acta Crystallogr., Sect. C: Cryst. Struct. Commun.*, 2000, vol. 56, p. 7.
42. Yamanaka, M., Uekusa, H., Ohba, S., et al., *Acta Crystallogr., Sect. B: Sctruct. Sci.*, 1991, vol. 47, p. 344.
43. Luo, M., Wang, L., and Zhang, J.C., *Acta Crystallogr., Sect. E: Struct. Rep. Online*, 2014, vol. 70, m27.
44. Kozlevcar, B., Murn, A., Podlipnik, K., et al., *Croat. Chem. Acta*, 2004, vol. 77, p. 613.
45. Davey, G. and Stephens, F.S., *J. Chem. Soc. A*, 1970, p. 2803.
46. Zhang Shi-Guo, Liu Qi-Sheng, and Shi Jing-Min, *Acta Crystallogr., Sect. E: Struct. Rep. Online*, 2007, vol. 63, p. m2082.
47. Uekusa, H., Ohba, S., Tokii, T., et al., *Acta Crystallogr., Sect. B: Struct. Sci.*, 1992, vol. 48, p. 650.
48. Kozlevcar, B., Lah, N., Zlindra, D., et al., *Acta Chim. Slov.*, 2001, vol. 48, p. 363.
49. Nefedov, S.E., Kushan, E.V., Yakovleva, M.A., et al., *Russ. J. Coord. Chem.*, 2012, vol. 38, p. 224.
50. Denisova, T.O., Amel'chenkova, E.V., Pruss, I.V., et al., *Russ. J. Inorg. Chem.*, 2006, vol. 51, p. 1020.
51. Spek, A.L., Spee, M., and van Koten, G., *CSD Communication (Private Communication)*, 2005.
52. Perova, E.V., Yakovleva, M.A., Baranova, E.O., et al., *Russ. J. Inorg. Chem.*, 2010, vol. 55, p. 714.

53. Fontanet, M., Rodriguez, M., Fontrodona, X., et al., *Chem.-Eur. J.*, 2014, vol. 20, p. 13993.
54. Cotton, F.A. and Walton, R.A., *Multiple Bonds between Metal Atoms*, Oxford: Clarendon, 1993.
55. Sidorov, A.A., Aleksandrov, G.G., Pakhmutova, E.V., et al., *Izv. Akad. Nauk. Ser. Khim*. 2005, p. 581.
56. Lee, D., Hung, P.-L., Spingler, B., and Lippard, S.J., *Inorg. Chem.*, 2002, vol. 41, p. 521.
57. Rakitin, Yu.V., Larin, G.M., and Minin, V.V. *Interpretatsiya spektrov EPR koordinatsionnykh soedinenii* (Interpretation of the ESR Spectra of Coordination Compounds), Moscow: Nauka, 1993.
58. Polunin, R.A., Kolotilov, S.V., Kiskin, M.A., et al., *Eur. J. Inorg. Chem.*, 2010, p. 5055.
59. Litvinenko, A.S., Mikhalyova, E.A., Kolotilov, S.V., and Pavlishchuk, V.V., *Theor. Experim. Chem.*, 2010, vol. 46, p. 422.
60. Programma Mjöllnir. https://sites.google.com/site/mjollnirmagn/.
61. Husebye, S., Kato, M., Maartmann-Moe, K., et al., *Acta Chem. Scand.*, 1994, vol. 48, p. 628.
62. Novotortsev, V.M., Rakitin, Yu.V., Nefedov, S.E., and Eremenko, I.L., *Izv. Akad. Nauk. Ser. Khim.* 2000, p. 437.
63. Zhu, L., Chen, X., Zhao, Q., et al., *Z. Anorg. Allg. Chem.*, 2010, vol. 636, p. 1441.
64. Cortijo, M., Delgado-Martinez, P., Gonzalez-Prieto, R., et al., *Inorg. Chim. Acta*, 2015, vol. 424, p. 176.
65. Pang, Y., Tian, D., Zhu, X.-F., et al., *CrystEngComm*, 2011, vol. 13, p. 5142.
66. Shi, Q., Sun, Y., Sheng, L., et al., *Inorg. Chim. Acta*, 2009, vol. 362, p. 4167.
67. Zhao, J., Wang, Y., Dong, W., et al., *Chem. Commun.*, 2015, vol. 51, p. 9479.

Translated by Z. Svitanko